July 2019

Thermal Response in a Field Oriented Controlled Three-phase Induction Motor

Niyem Mawenbe Bawana
University of South Florida, bawana12@gmail.com

Thermal Response in a Field Oriented Controlled Three-phase Induction Motor

by

Niyem Mawenbe Bawana

A thesis submitted in partial fulfillment
of the requirements for the degree of
Master of Science in Electrical Engineering
Department of Electrical Engineering
College of Engineering
University of South Florida

Major Professor: Wilfrido Moreno, Ph.D.
Chung Seop Jeong, Ph.D.
Frank Pyrtle, Ph.D.

Date of Approval:
July 11, 2019

Keywords: vector control, thermal protection, overheating, thermal model

DEDICATION

To my wife,

Djobelaba Balaka

and

my boys

Prince David Bawana and James David Jr Bawana

ACKNOWLEDGMENTS

I want to thank the Fulbright board and the U.S Department of Education for all the support they have given me to study at the University of South Florida.

I would like to thank Dr. Ralph Fehr for being a source of motivation for me. Due to his experience in power field, I approached him after his electrical power distribution class I was taking and shared the first research ideas of this project with him. He gave me his full support and agreed to co-supervise this work with Dr Wilfrido Moreno. While he could not continue this journey with me because of health issues, I would like to express to him my deepest gratitude. I also appreciate that Dr. Wilfrido Moreno took the whole responsibility of this research and guided me through the end. Not only he was an academic mentor for a student I was, but he also guided and supported me through many other life challenges. May God bless Dr. Wilfrido Moreno for all his unconditional support and sacrifices

This thesis has also significantly benefited from the many outstanding reviews of Dr. Frank Pyrtle and Dr. Chung Seop Jeong. I appreciate the feedback received from these professors and would like to thank them for their time, attention and energy they have invested in this work.

I want to express my appreciation to my wife, Djobelaba Balaka, our boys, Prince David and James David Jr Bawana and my family and friends for their continued support throughout this journey. I would also like to say thank you to all those known or unknown persons whose advice, lives and words have positively influenced me during the realization of this work.

Finally, my deepest gratitude goes to God for all what he has done in my life so far.

TABLE OF CONTENTS

LIST OF TABLES

LIST OF FIGURES

ABSTRACT

The research conducted at the department of Electrical Engineering of the University of South Florida campus in Tampa only covers the electrical aspect of electric drives. However, the performance of electric machinery is significantly impacted by temperature variation. The literature review shows three main control techniques in use today in electric drives namely, Scalar control, Direct Torque control and Field Oriented control.

This thesis presents a temperature rise of rotor bars, stator winding, stator core and stator frame in a running three phase field-oriented controlled induction machine. A literature search shows that none of research has been carried out to investigate a thermal response of a field-oriented controlled induction motor. With this motivation, we were able to implement a lumped parameters thermal model of a three-phase field-oriented IM in MATLAB Simulink, which allows us to determine that rotor bars have the highest temperatures rising to 84 degrees Celsius. This confirms that rotors bars are the hottest part of a running IM as stipulated in literature.

CHAPTER 1: INTRODUCTION

1.1 Introduction

Induction motors are used widely nowadays, ranging from small domestic motors applications to large scale industrial applications. Typical applications of induction motors include pumps, fans, compressors, mills, shredders, extruders, de-barkers, refiners, cranes, conveyors, chillers, crushers, blowers and wind generators. The reason for this high interest for induction motors is due to their robustness, their low costs and the low-cost maintenance required while under operation.

Despite their enhanced reliability and construction simplicity, induction motors failure is a major concern and increases aggressively for example in pulp and paper. One of the major concern of motors failure is due to thermal risks during the motor's operation. The excessive accumulation of heat on an induction motor may cause severe thermal stress and even result in the machine burnout. Downtime in some industry can be very expensive therefore a need for proper machine thermal protection is required to minimize the diverse type of losses such as economical or power and ensure personnel safety.

Figure 1.1 Three phase IM. [6]

1.2 Literature Review

During induction motor operation, losses occur and these result in thermal stress or temperature increase in the motor. This situation can lead to economic losses and motor burnout.

It has been reported that 3 to 4% of induction motors failure occurs yearly due to overheating conditions [10].

Overload relays are inefficient for thermal protection of variable speed induction motor operating at low speed. The oversizing strategy is generally used to alleviate the overheating of an induction motor. Unfortunately, this technique is not appropriate under low-speed operation. In addition, it induces additional costs [1].

Initially, induction motors were built to be used for constant speed applications. The recent development in power electronics and control systems made it easier to use induction motors in applications at variable speed. Vector control technique for speed control of induction motors has

facilitated the use of an induction motor within a wide range of speeds. This technique simplifies the complexity of the control of an induction motor. The technique is like what volt/hertz technique is for DC motors. The number of applications using vector control has shown an important increase in recent years. Since high temperature beyond the predicted values can cause a motor failure and result in economic losses, it is hence highly recommended to predict the temperature rise in the motors accurately.

During the last decades, many researchers have delved into thermal modeling of induction motors leading to several models which help to predict the temperature in the complex structure of induction motors. Bogglieth et al. developed a simple model based on thermal resistance. This simplified model is intended for self-cooled induction motors and is useful for steady-state analysis [3]. A much more precise analysis of an induction motor thermal model requires finite element analysis (FEA). While modern computers are equipped with powerful CPUs, FEA technique is a time-consuming technique and can lead in some cases to computer crash. A need for less computation intensive technique is then required while willing to perform a quick and reliable thermal analysis. A thermal model analysis using lumped parameters is established as an accurate way of performing temperature prediction in an induction motor [9].

1.3 Research Motivation and Objectives

The early use of induction machines was realized in non-controllable situations. But with the advances realized in the power electronics field and the improvement of control techniques, induction machines are frequently used today in controllable applications. Different control techniques are being implemented with induction machines such as scalar control and vector control. The vector control makes it easier to control an induction motor with the same approach as scalar control does it with DC motors.

With the increase demand of induction motors in modern applications using vector control, the need of an accurate estimation of their thermal response is important to ensure their protection and reduce energy losses and motor failure while in service. This thesis is an attempt to implement an estimate of the thermal response of a three-phase induction machine under vector control.

The specific objectives of this thesis are formulated as follows:

- Describe a three-phase induction motor thermal model using lumped parameters approach;
- Estimation of the temperature-rise in three-phase induction motor main parts under vector control using lumped parameters model.

1.4 Organization of this Thesis

In chapter 2 of this thesis, the theory of induction motor is described. A focus is put on electrical and mechanical aspects. The theory of vector control and the algorithm of this technique is also described. In chapter 3, the thermal model of induction motor using lumped parameters approach is first presented and followed by losses calculation and the deduction of the temperature rise in the motor mains parts. Simulations results are presented in chapter 4 and chapter 5 gives a summary of the thesis with recommendations for future research.

CHAPTER 2: THEORY OF INDUCTION MOTOR AND VECTOR CONTROL

2.1 Introduction

Induction motors advantages over the other type of electrical machines make them more attractive in modern world applications. It is therefore mandatory to understand the basic formulations regarding this type of electromechanical device. This chapter therefore focuses on the electrical and mechanical aspect of IM and a commonly used control technique, F.O.C which is frequently used in variable frequency applications with IM.

2.2 Principle of Operation of IM

This section delves into the operation principle of the IM. Each part of the motor contributes to its operation in the following steps:

- A rotating magnetic field is initiated in the stator when the supply electrical source is connected to the IM;
- The rotor which is initially in a stationary state cuts the revolving field, but an electromagnetic induction produces an e.m.f. in the IM;
- The rotor conductor is then short-circuited and current starts flowing through them;
- The rotor finally starts rotating.

2.3 Electrical Model

This section focusses on electrical modeling of IM. The per phase representation for the steady state description of the IM is reviewed, followed by the dq description of the machine.

2.3.1 Per Phase Equivalent Circuit

The per phase representation as shown on figure 2.1 is a simplified electrical circuit which represents the stator, the core and the rotor of an IM. This electrical circuit is used to deduce useful data of the IM while running under steady state.

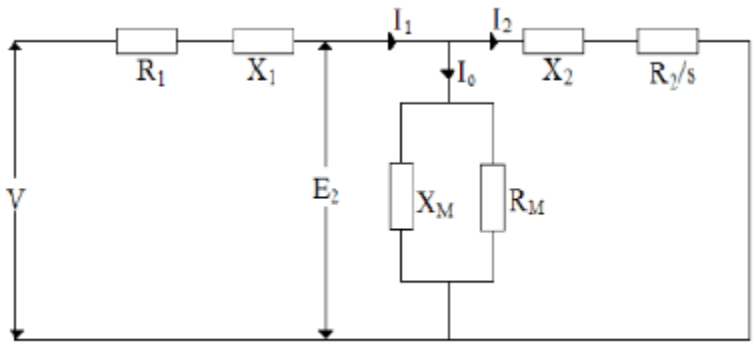

Figure 2.1 Equivalent circuit of IM [9]

The following electrical properties are derived from the per phase representation.

The stator impedance equation is given by:

$$Zs = Rs + jXs \qquad 2.1$$

The following equation gives the rotor's impedance:

$$Zr = \frac{Rr}{s} + jXr \qquad 2.2$$

The magnetizing impedance value is:

$$ZM = (RM * jXM)/(RM + jXM) \qquad 2.3$$

2.3.2 Dynamic dq Model

In a transient state of an induction motor, the dq model allows an accurate representation of the machine. The dynamic model was introduced by R.H.Park in the 1920s and was named after his name as Park's transformation.

R.H Park's transformation is one of the best set of equations which describes accurately an induction motor. This transformation can be written as follow:

$$\begin{bmatrix} f_q \\ f_d \\ f_o \end{bmatrix} = \begin{bmatrix} \cos\theta & \cos\left(\theta - \frac{2\pi}{3}\right) & \cos\left(\theta + \frac{2\pi}{3}\right) \\ \sin\theta & \sin\left(\theta - \frac{2\pi}{3}\right) & \sin\left(\theta + \frac{2\pi}{3}\right) \\ \frac{1}{2} & \frac{1}{2} & \frac{1}{2} \end{bmatrix} \begin{bmatrix} f_a \\ f_b \\ f_c \end{bmatrix} \qquad 2.4$$

The above transformation shows how three-phase variables of an induction motor are expressed in the dq reference frame. These variables could be interpreted as the current, voltage of flux leakage. The reduction of axes from 3 to 2 in a Park transformation induces a huge simplification while performing calculations.

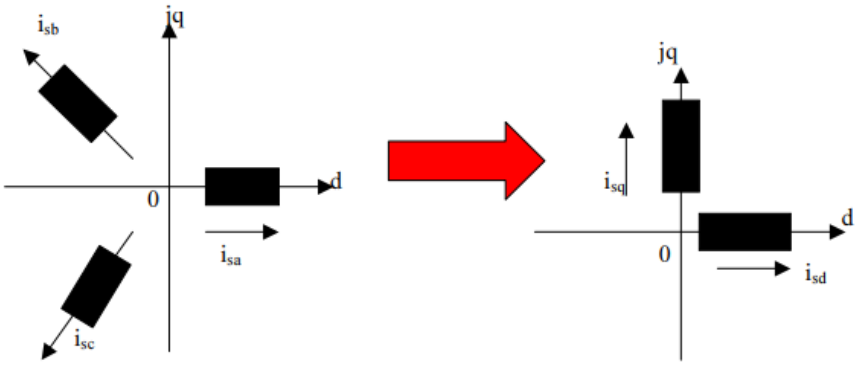

Figure 2.2 Park transformation from abc to dq frame [4]

The governing equations describing an induction motor are of two orders: electrical and mechanical. We will focus on a three-phase balanced case.

The voltage of the dynamic representation is given by:

$$v_{qs} = R_s i_{qs} + p\lambda_{qs} + \omega\lambda_{ds} \quad 2.5$$

$$v_{ds} = R_s i_{ds} + p\lambda_{ds} - \omega\lambda_{qs} \quad 2.6$$

$$v_{qr} = 0 = R_r i_{qr} + (\omega - \omega_r)\lambda_{dr} + p\lambda_{qr} \qquad 2.7$$

$$v_{dr} = 0 = R_r i_{dr} + (\omega - \omega_r)\lambda_{qr} + p\lambda_{dr} \qquad 2.8$$

The flux calculation is performed as followed:

$$\lambda_{qs} = L_{ls} i_{qs} + L_m(i_{qs} + i_{qr}) \qquad 2.9$$

$$\lambda_{ds} = L_{ls} i_{ds} + L_m (i_{ds} + i_{dr}) \qquad 2.10$$

$$\lambda_{qr} = L_{lr} i_{qr} + L_m (i_{qs} + i_{qr}) \qquad 2.11$$

$$\lambda_{dr} = L_{lr} i_{dr} + L_m (i_{ds} + i_{dr}) \qquad 2.12$$

2.4 Mechanical Equations

The electromagnetic torque and the load torque are defined respectively by equations 2.13 and 2.14.

$$T_e = \frac{3P}{4} \frac{L_m}{(L_{lr} + L_m)} (\lambda_{qr} i_{dr} - \lambda_{dr} i_{qr}) \qquad 2.13$$

$$T_e - T_l = \frac{2J}{P} p \omega_r \qquad 2.14$$

The difference between the synchronous speed and the actual rotating speed of the IM motor leads to a quantity called slip:

$$s = \frac{Ns - N}{Ns} \qquad 2.15$$

$$Ns = \frac{120 f}{p} \qquad 2.16$$

The angular velocity ω and the displacement Θ are related by the following equation:

$$\theta = \int \omega dt \qquad 2.17$$

2.5 Theory of Vector Control

2.5.1 Overview of Vector Control

Vector control also known as field-oriented control is a technique first developed by Blaschke (1971-1973). FOC makes easier the use of IM in VFD and allows an analogy in control scheme between AC motors and DC motors.

Two fundamental ideas govern the principle of FOC.

First, IM is modeled using two types of currents instead of the traditional three-phase currents which are applied to the machine. The direct (i_d) and quadrature (i_q) currents. The direct

component is in phase with the stator flux while the quadrature component is 90 degrees shifted from the direct component. The direct current modification helps to control the stator flux while the quadrature current controls the torque.

Secondly, a well-chosen reference permits the transformation of sinusoidal values into constants values. This facilitates the use of the conventional PI controllers to perform the machine control as in the case of DC motor.

2.5.2 F.O.C Algorithm

- The first step is to measure the currents in abc frame.
- Then apply Clarke transformation. This turns the set of three-phase equations onto the two-axis system. But the equations are still time varying equations.
- We now calculate the rotor flux.
- A rotation permits to align the two-axis coordinates with the rotor flux.
- The application of Park transformation allows us to get ready of the time in the equations obtained after Clarke transformation.
- The difference between the estimated flux value and the flux reference value gives the error.
- A PI controller is used to generate id^* using the flux error.
- id^* and iq^* are converted back to ia^*, ib^*, and ic^*.
- ia^*, ib^*, ic^* and ia, ib, ic are compared using hysteresis comparator to generate inverter gate signal.

CHAPTER 3: THERMAL MODEL, LOSSES, AND TEMPERATURE CALCULATION

3.1 Introduction

In this chapter, we will present the thermal model of the IM based on lumped parameters. The IM is divided into 10 parts as shown on figure 3.1which simplifies the complex structure of the motor.

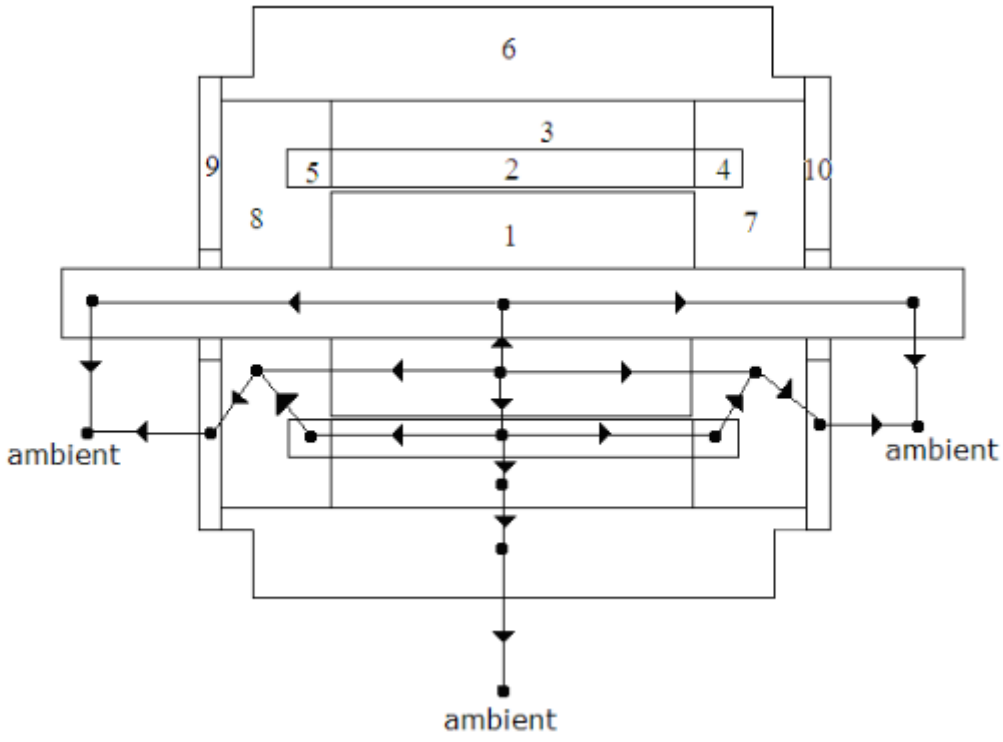

Figure 3.1 Longitudinal cross section of IM showing the main elements of the thermal model [9]

3.2 Lumped Parameters Thermal Model of IM

On figure 3.2, the electrical equivalent circuit of the IM and its thermal behavior is summarized. Rij represents the thermal resistance between two adjacent parts, and can be viewed as the opposition to heat transfer from one part to the adjacent part. The Ci represents the thermal capacitances of the part i. This characterize the ability of the piece of the IM to store heat during its operation time.

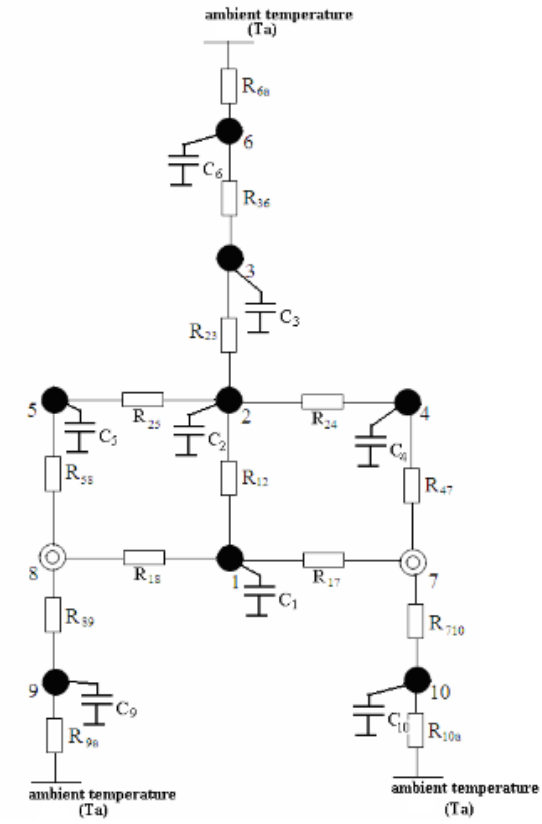

Figure 3.2 Thermal model of IM [9]

In steady state, the thermal capacitance is usually:

$$C_{th} = \rho * Cp * V \quad 3.1$$

ρ= density of the material

V= volume of the element

Cp= specific heat capacity of the material.

In transient situation where n nodes are linked to each other through thermal resistances Rij, the following equation is used:

$$\mathrm{Ci} * \frac{\mathrm{dTi}}{\mathrm{dt}} = \mathrm{Pi} - \sum_{j=1}^{n} \frac{(Ti - Tj)}{Rij} \qquad 3.2$$

Ti=node temperature rise.

Pi= heat generation at node i.

3.3 Determination of Losses in IM

In this section, we elaborate on the major type of electrical losses in an IM. These losses are mainly due to joule's law. The flow of current in a material induces a temperature gradient and heat dissipation.

3.3.1 Stator Copper Losses

Most wiring in a stator of an IM are made of copper and when a current flow in these materials, losses are evaluated as shown in equation 3.1.

$$P_{scl} = 3I_S^2 R_S \quad 3.3$$

3.3.2 Rotor Copper Losses

The rotor of an IM is made of copper and the losses in this part of the motor are calculated by equation 3.2.

$$P_{rcl} = 3I_r^2 R_r \quad 3.4$$

3.3.3 Core Losses

The core of an IM is also a part where most losses occur. Equation 3.3 shows the estimation of the losses in the core of the motor.

$$P_{core} = 3\left(\frac{E_2^2}{R_c}\right) \qquad 3.5$$

$$E_2 = I_S Z_p \qquad 3.6$$

3.4 The Heat Balance Equations

The mathematical equations describing the heat balance equation in the induction motor is derived from the general energy conservation relationship as follows:

(Rate of energy stored within system)=(heat flow rate into system)-(heat flow rate out of system)+(rate of heat generated within system) 3.7

By assuming that the induction motor used in our research is a stationary system, equation 3.5 is simplified in the following equation:

$$\rho * Cp * P * V * dT/dt = Q_{in} - Q_{out} + Q_{gen} \quad 3.8$$

Equation 3.6 is only valid under the following assumptions:

- the temperature distribution is uniform;
- the induction motor physical properties are constant within some boundary conditions.

3.5 Heat Transfer Methods

Energy losses in the induction motor occur by mean of traditional heat transfer methods such as conduction, convection, radiation or a set of combination of the primary methods listed above.

3.5.1 Conduction

When energy is transferred from a more energetic particle of a substance to adjacent less energetic one, the phenomenon is called conduction. Conduction phenomenon can occur in solid, liquid or gases matters. Fourier's law of heat is written as follows:

$$Q_{cond} = -KA\ dT/dx \quad 3.9$$

The conduction resistance is derived as:

$$R_{cond}=\Delta T/Q_{cond}=\Delta x/KA \quad 3.10$$

3.5.2 Convection

When energy is transferred between a solid surface and an adjacent liquid or gas, the phenomenon is named convection. The mathematical equation governing convection is named as Newton's law of cooling:

$$Q_{conv}=hAS\ (T_S-T_\infty) \quad 3.11$$

The convection resistance is derived as:

$$R_{conv}=1/(hAS) \quad 3.12$$

3.5.3 Radiation

The process of radiation is dependent on the system's temperature. Stefan-Boltzmann's Equation expresses the radiation process as follows:

$$Q_{rad}=\varepsilon\sigma_{SB}\ (T_1^4-T_2^4) \quad 3.13$$

The radiation phenomenon is neglected in our analysis because the temperature of the induction motor is assumed not to be high enough to simulate radiation.

3.6 Temperature Rise Calculation in an IM

The temperature rise in an induction motor originates from the accumulation of heat due to losses. The following losses can be categorized:

- Losses dependent on the motor current: stator winding losses, rotor bars losses, and stray-load losses;
- Losses independent on current: core losses due to eddy current and hysteresis, friction and winding losses.

In this thesis, temperature estimation based on a thermal model using lumped parameters is performed. The following differential equations govern the calculation of temperature at several points defined by the lumped thermal model of the figure 3.1:

$$C_1 \frac{dT_1}{dt} = P_{rol} - (G_{12} + G_{17} + G_{18})T_1 + G_{12}T_2 + G_{17}T_7 + G_{18}T_8 \quad 3.14$$

$$C_2 \frac{dT_2}{dt} = P_{scl,sw} - (G_{23} + G_{24} + G_{25})T_2 + G_{23}T_3 + G_{24}T_4 + G_{25}T_5 \quad 3.15$$

$$C_3 \frac{dT_3}{dt} = P_{core} - (G_{23} + G_{36})T_3 + G_{23}T_2 + G_{36}T_6 \quad 3.16$$

$$C_4 \frac{dT_4}{dt} = P_{scl,ew} - (G_{24} + G_{47})T_4 + G_{24}T_2 + G_{47}T_7 \quad 3.17$$

$$C_5 \frac{dT_5}{dt} = P_{scl,ew} - (G_{25} + G_{58})T_5 + G_{25}T_2 + G_{58}T_8 \quad 3.18$$

$$C_6 \frac{dT_6}{dt} = P_{r-frame} - (G_{36} + G_{6a})T_6 + G_{36}T_3 + G_{6a}T_a \quad 3.19$$

$$C_7 \frac{dT_7}{dt} = P_{capair} - (G_{47} + G_{17} + G_{710})T_7 + G_{47}T_4 + G_{17}T_1 + G_{710}T_{10} \quad 3.20$$

$$C_8 \frac{dT_8}{dt} = P_{capair} - (G_{58} + G_{18} + G_{89})T_8 + G_{58}T_5 + G_{18}T_1 + G_{89}T_9 \quad 3.21$$

$$C_9 \frac{dT_9}{dt} = P_{s-frame} - (G_{89} + G_{9a})T_9 + G_{89}T_8 + G_{9a}T_a \quad 3.22$$

$$C_{10} \frac{dT_{10}}{dt} = P_{s-frame} - (G_{710} + G_{10a})T_{10} + G_{710}T_7 + G_{10a}T_a \quad 3.23$$

The Ci parameters are the thermal capacitance associated to the 10 parts of the motor as defined in the lumped parameter model depicted by figure 3.1. A thermal capacitance of a particular piece is the product of the following characteristics of that part: the thermal conductivity of the materials, the specific heat and the volume. Table 3.1. summarizes the properties of materials used by the manufacturer of the used motor.

Table 3.1 Physical properties of the materials in the IM [9]

Material	Thermal conductivity (W/m.C)	Density (Kg/m^3)	Specific heat (J/Kg.C)
Iron	58	7850	420
Aluminum	222	2790	833
Steel	35	7770	460
copper	388	8933	385
Ambientair	0.02624	1.127	1007

CHAPTER 4: SIMULATIONS

4.1 Introduction

This chapter presents MATLAB/SIMULINK model and the simulations results of a three-phase IM temperature estimation of its main parts as described by the lumped parameters model.

4.2 Simulink Model

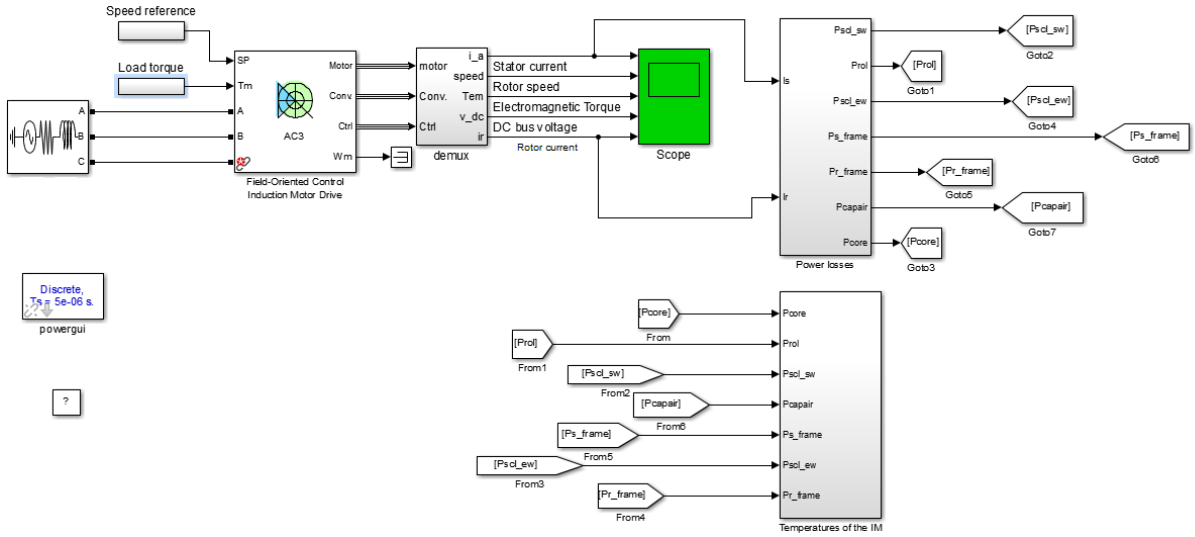

Figure 4.1 MATLAB/SIMULINK block diagram

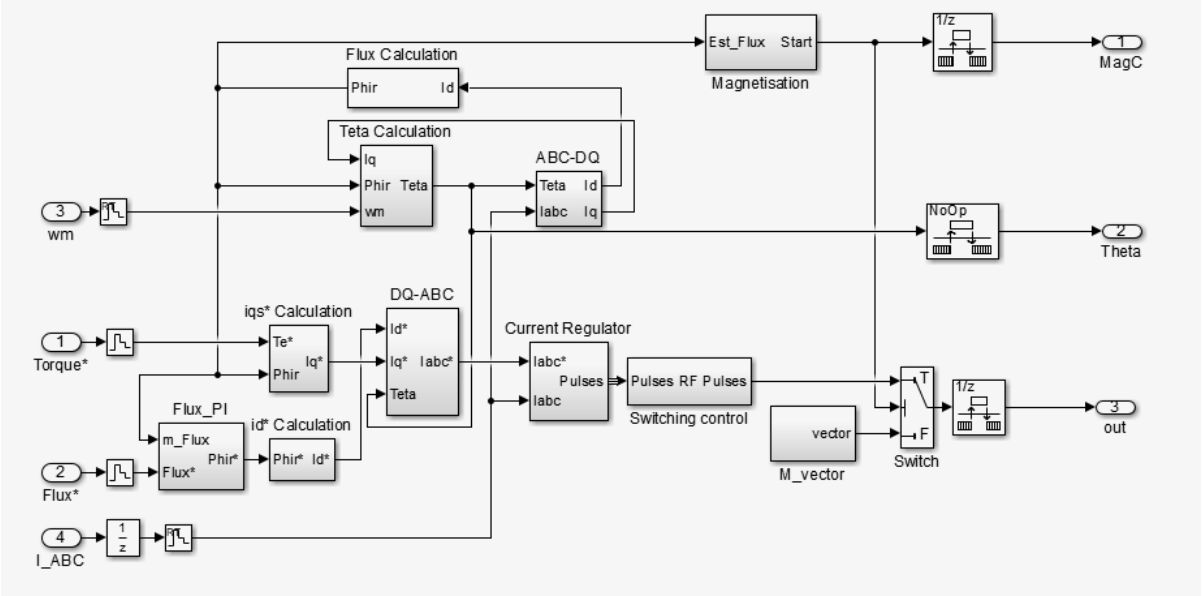

Figure 4.2 F.O.C implementation block diagram

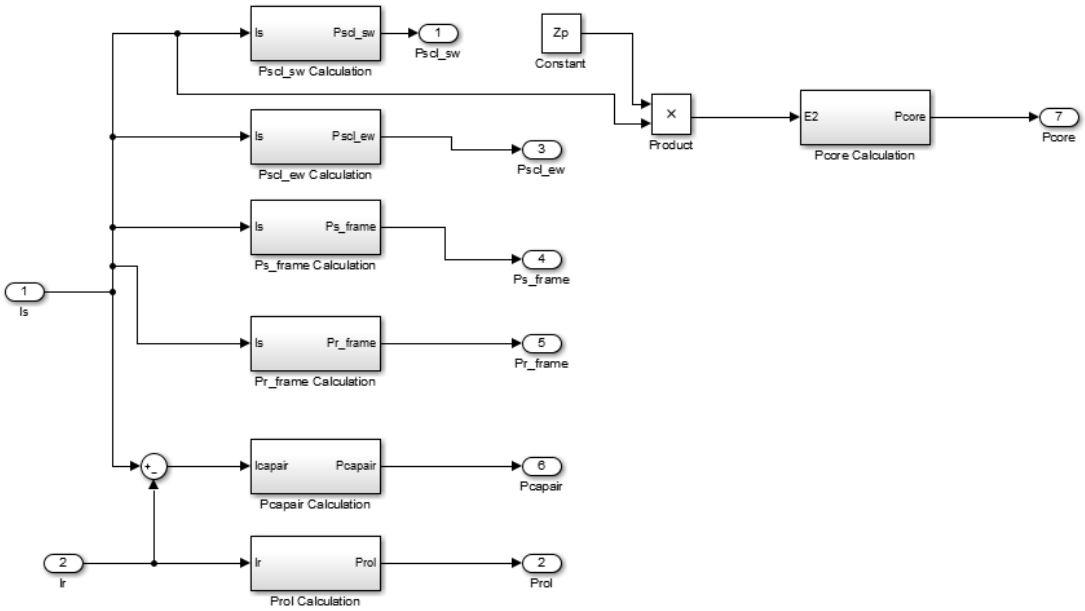

Figure 4.3 Power losses calculation

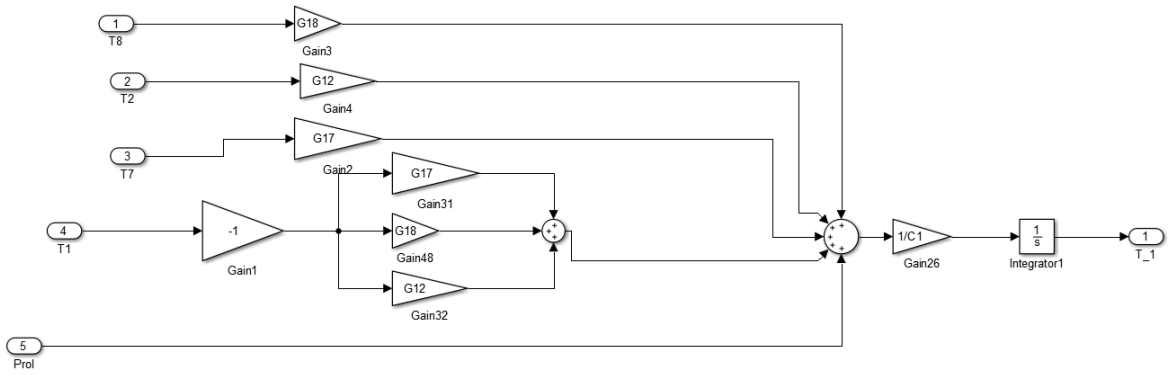

Figure 4.4 Example of temperature calculation in rotor bars

4.3 Machine Parameters

The table 4.1 summarizes the motor parameters of the equivalent circuit of figure 2.2. All the IM dimensions and specifications are summarized in Table 4.2.

Table 4.1 Equivalent circuit parameters of the used IM

parameter	Value (Ω)
Rs	4.1667
Rr	3.33
Xs	3.33
Xr	7.08
XM	111.3

Table 4.2 Dimensions and the specifications of the used IM [modified from [9]]

Parameters	*Value*	*Parameters*	*value*
power	1.5 KW	Stator inductances	4.72 Ω
Rotor speed	2840 r/min/3405 r/min	Magnetizing inductance	111.3 Ω
Phase number	3	Rotor inductance	7.08 Ω
Voltage	220-380/240-420 V		
Current	5.9-3.4/5.4-3.08 A		
frequency	50 Hz / 60 Hz		
Stator resistance	4.167 Ω		
Magnetizing resistance	1187.48 Ω		
Rotor resistance	3.333 Ω		
Slot number	18	Stator length	82 mm
Stator diameter	131.5 mm	Rotor length	82 mm
Housing diameter	145 mm	Motor length	208.5 mm
Stator bore	72.5 mm	End winding extension	50 mm
Tooth width	5 mm	End winding inner diameter	72.5 mm
Slot depth	16 mm	End winding outer diameter	104.5mm
Air gap	0.5 mm	Bearing diameter	52 mm
Rotor diameter	71.5 mm	Bearing width	15 mm
Shaft diameter	29.5 mm		

4.4 Simulation Results

In the following section, we present the simulation results. The characteristics of the running IM such as the stator current, the rotor speed and the motor torque are extracted and temperatures variation of four major parts of the IM are also shown.

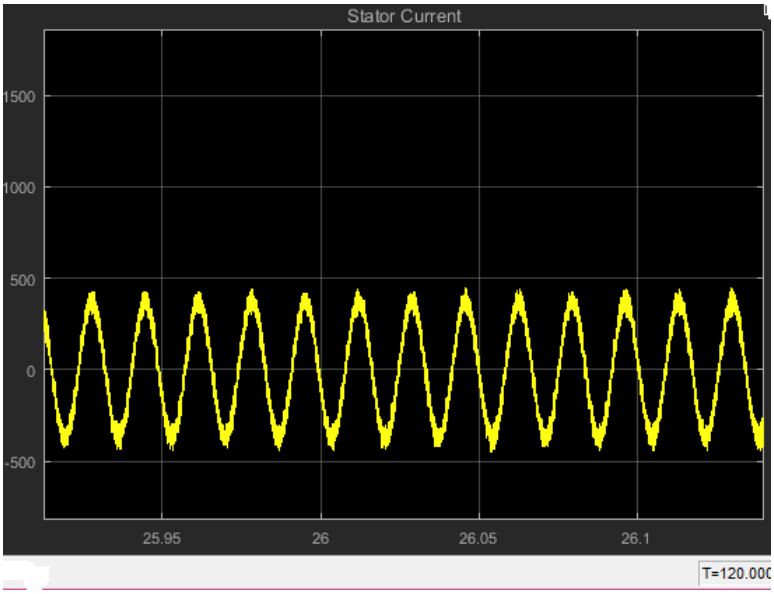

Figure 4.5 Stator current of the IM

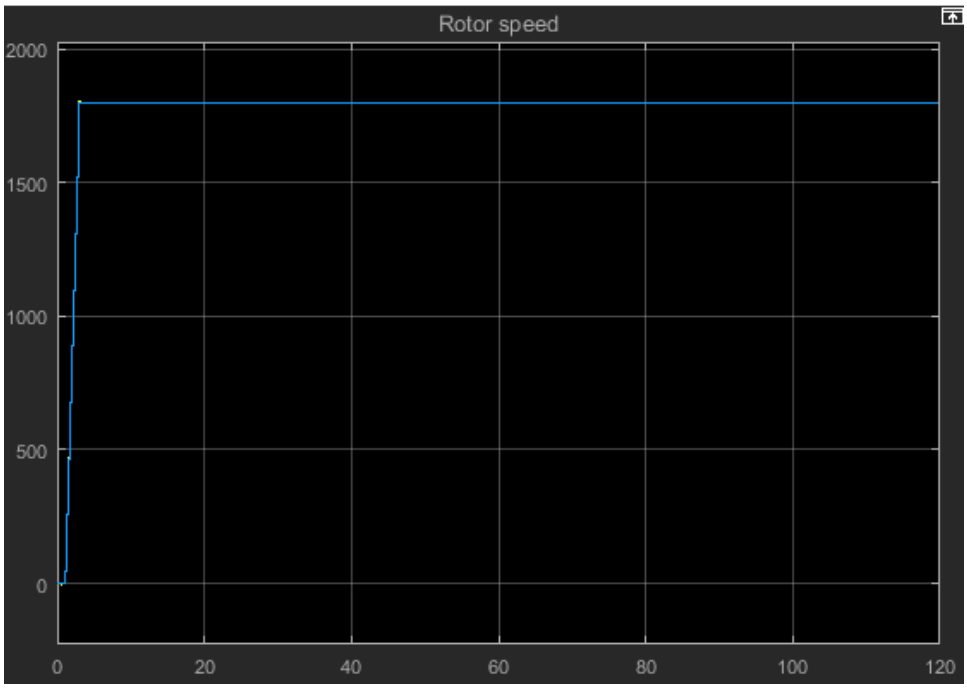

Figure 4.6 Rotor speed of the IM

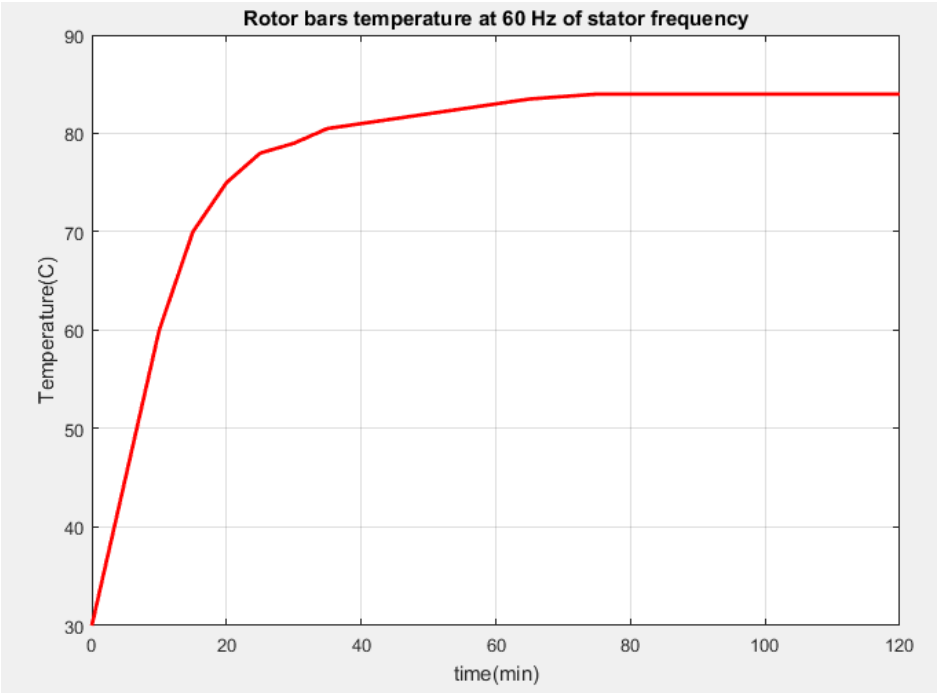

Figure 4.7 Rotor bars temperature

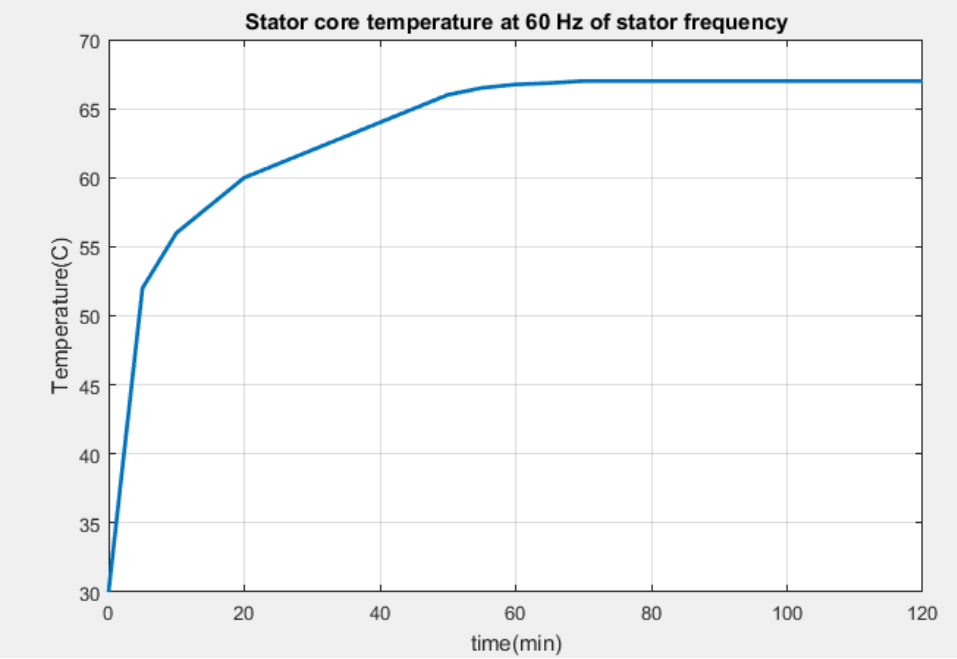

Figure 4.8 Stator core temperature

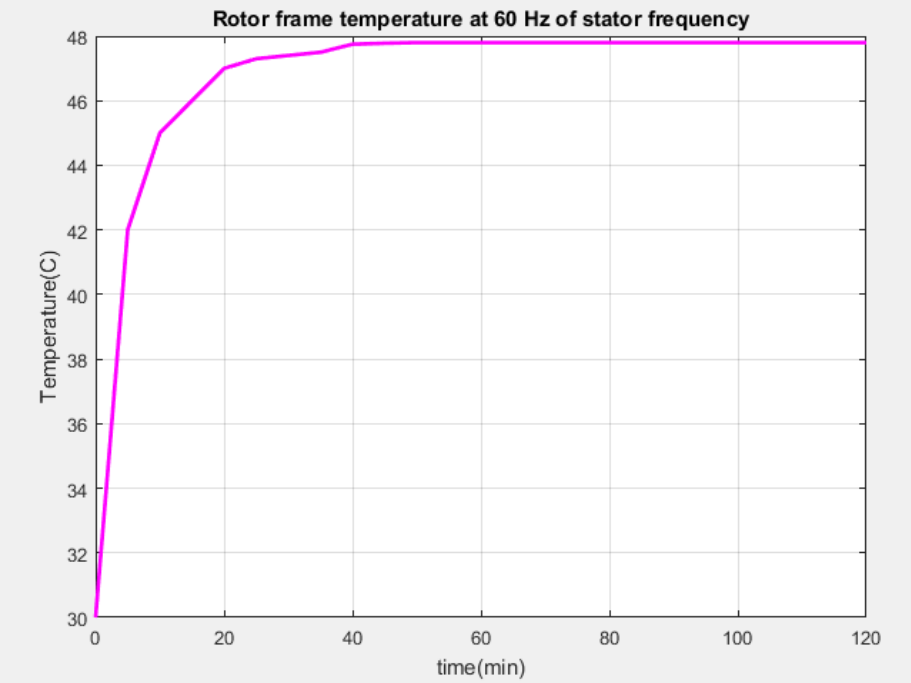

Figure 4.9 Rotor frame temperature

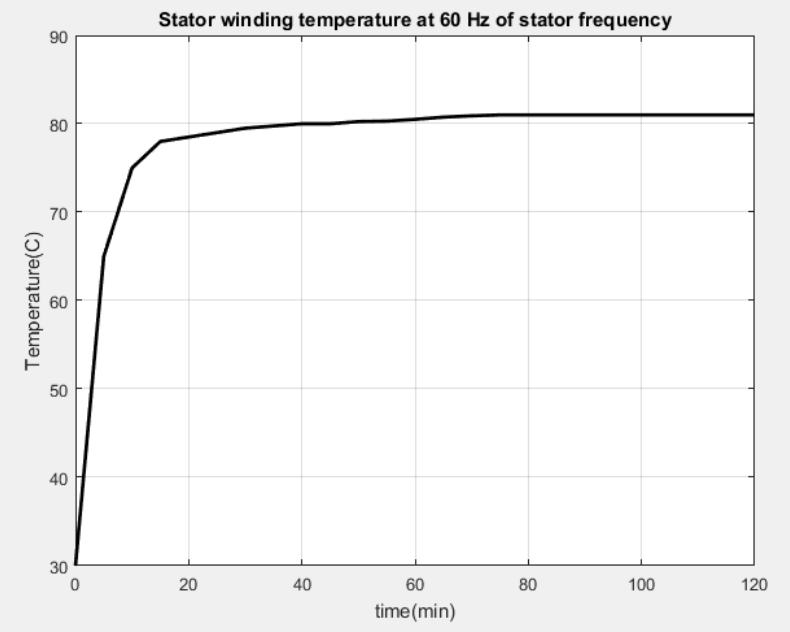

Figure 4.10 Stator winding temperature

4.5 Comments on Simulation Results

The simulations were performed for 120 minutes. We only present in this thesis the electromagnetic characteristics and the temperature estimation of four mains part of the IM.The extracted results show the stator current, the rotor speed for as the electrical and mechanical quantities. The speed of the motor, figure 4.6, goes quickly through a short transient period and then stabilizes at the synchronous speed of 1800 rpm. The stator current figure 4.5 and the IM torque figure 4.7 which are both sinusoidal confirm the nature of a three-phase balanced signal applied to the motor. When the IM is running, the power loss induces an increase in the whole device. This thesis has divided the motor in ten lumped parts and only the temperature of four major part are simulated. Figures 4.7, 4.8, 4.9 and 4.10 show respectively the temperature evolution in the rotor bars, the stator core, rotor frame and the stator winding. In each case, the temperature first increases and then stabilizes. The highest temperatures were recorded in the rotor

bars with a maximum of 80 degrees Celsius and shows that this part of the machine is the hottest area.

CHAPTER 5: CONCLUSION

5.1 Conclusion

This thesis reviewed the various models of the IM such as electrical, mechanical and thermal. An attention was dedicated to the temperature estimation in the IM due to the temperature impact on the motor efficiency. An implementation of temperature simulation of different sections of the IM was conducted using lumped parameters model developed in [9]. The simulation results identify that the rotor bars are the hot area of the motor. This research also opens doors to a potential energy saving in a field oriented IM and is an opportunity to extend the life time of the motor which is usually reduced due to overheating.

Due to time limit and resources unavailability, the work carried out in this thesis is incomplete. Therefore, the following section is dedicated to formulating some recommendations to improve this research outcomes in future.

5.2 Recommendation and Future Work

This work relied exclusively on simulation method and the author is willing to conduct experimental measurements to validate the results.

Also, in future work, the effect of temperature on the IM parameters is to be considered.

REFERENCES

[1] Z. Gao, “Sensorless Stator Winding Temperature Estimation for Induction Machines” Ph.D. dissertation, December 2006.

[2] A. Bazzi, P. T.Kerein, “Review of Methods for Real-time Loss Minimization in Induction Machine.”

[3] B. K. Bose, “Modern power electronics and AC drives”, Prentice-Hall, Inc. ISBN 0-13-016743-6

[4] O. I. Okoro, “Dynamic Thermal Modelling of Induction Machine with Non-Linear Effects”, PhD dissertation Kassel University.

[5] H. Haq, M. H. Imran, H. I. Okumus and M. Habibullah, “Speed control of induction motor using FOC method,” *Int. J. Eng. Res. Appl.*, vol. 3, March 2015.

[6] https://www.theengineeringprojects.com/2016/09/introduction-induction-motor.html

[7] A. Boubaine, M. McCormick and W.F Low, "In-situ determination of thermal coefficients for electrical machines " *IEEE Trans. En. Conv.*, vol. 10, no. 3, 1995

[8] https://circuitglobe.com/power-flow-diagram-and-losses-of-induction-motor.html

[9] B. Omar, S. Hussain and A. Bilal, "Thermal performance analysis of induction machine", *in* International Journal of Heat and Technology, page:75-88, January 2012.

[10] A. Gedzurs and A. Sniders, “Induction motor stator winding thermal process research and modelling under locked rotor mode”, *Jelgava*, pp. 265–270, 2014.

[11] M. Maximini and K. Hans-Jurgen, “Determination of the absolute rotor temperature of squirrel cage induction machines using measurable variables,” vol. 19, pp. 34–39, 2004.

[12] S. Lee, T. G. Habetler, R. G. Harley, and J. G. David, “An e valuation of model-based stator resistance estimation for induction motor stator winding temperature monitoring,” *IEEE Trans. Energy Convers.*, vol. 17, 2002.

[13] Z. Gao, T. G. Habetler, R. G. Harley, and R. S. Colby, “A sensorless rotor temperature estimator for induction machines based on a current harmonic spectral estimation scheme,” *IEEE Trans. Ind. Electron.*, vol. 55, pp. 407–416, 2008.

[14] Y. A. Cengel, M. A. BOLES, "*Thermodynamics: an engineering approach"*, Fith. McGraw-Hill, 2006.

[15] H. Haq and M. Habibullah, “Speed control of induction motor using F.O.C method" no. April 2015.

[16] O.Badran, H.Sarhan, B.Alomour, "Thermal performance analysis of induction motor"

[17] A. H. Bonnett and G. C. Soukup, “Cause and analysis of stator and rotor failures in three-phase squirrel-cage induction motors,” *IEEE Trans. Ind. Appl.*, vol. 28, no. 4, pp. 921–937, Aug. 1992.

[18] D. Biswas, "Minimization of electrical losses in vector controlled induction machine drive", MS thesis, University of Windsor, 2013

APPENDIX A: NOMENCLATURE

IM : Induction Motor

v_{qs} : Q-axis stator voltage

v_{ds} : D-axis stator voltage

i_{qs} : Q-axis stator current

i_{ds} : D-axis stator current

i_{qr} : Q-axis rotor current

i_{dr} : D-axis rotor current

R_s : Stator resistance

R_r : Rotor resistance

R_M : Core resistance

P_{scl} : Stator copper losses

P_{rol} : Rotor bars losses

P_{core} : Core losses

R_{ij} : Thermal resistance

Q_{in} : Heat flow rate into system

Q_{out} : Heat flow rate out of system

Q_{gen} : Rate of heat generated within system

ρ : Density

C_p : Specific heat

T_i : Temperature in specific part of the IM as described in the lumped parameter model

V : Volume

Ci : Thermal capacitance of part i as described in the lumped model of the IM

A : Area

H : Convection heat transfer coefficient

K : Thermal conductivity

Gij : Thermal admittance

D : IM friction coefficient

J : IM inertia

s : Slip of the IM

P : Number of pair poles of the IM

APPENDIX B: COPYRIGHT PERMISSIONS

The permission below is for the use of figure 2.1 in chapter 2; figures 3.1, 3.2 and table 3.1 in chapter 3 and table 4.2 in chapter 4.

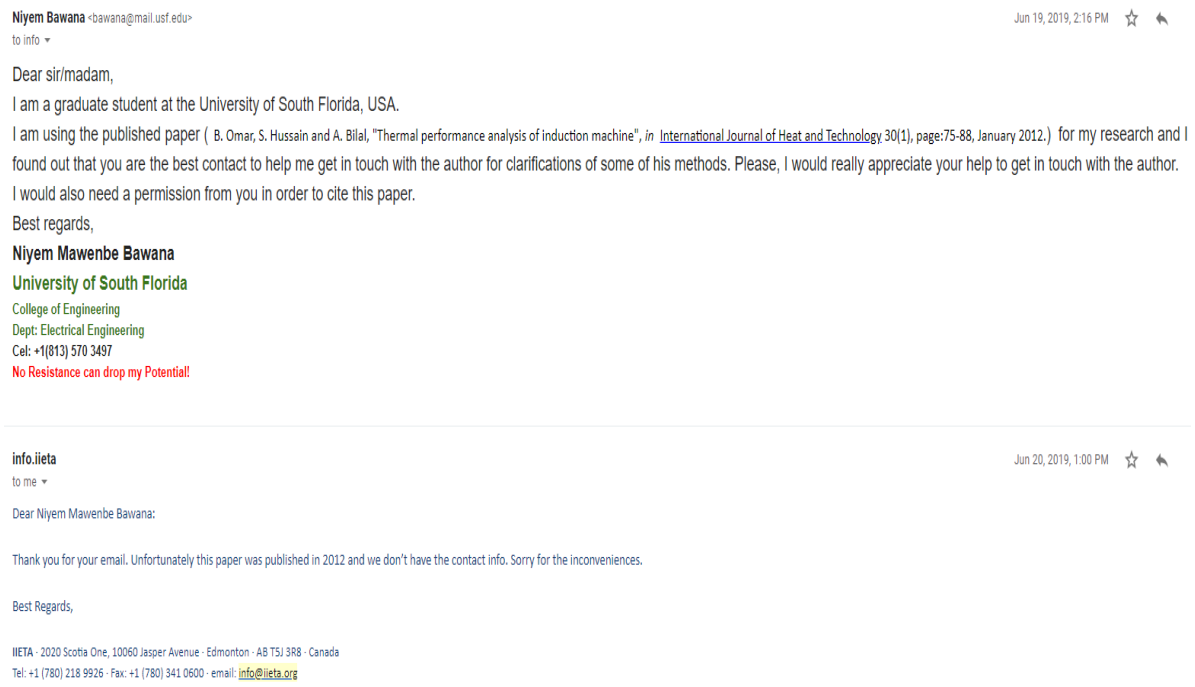

Niyem Bawana <bawana@mail.usf.edu> Jun 19, 2019, 2:16 PM

to info

Dear sir/madam,

I am a graduate student at the University of South Florida, USA.

I am using the published paper (B. Omar, S. Hussain and A. Bilal, "Thermal performance analysis of induction machine", *in* International Journal of Heat and Technology 30(1), page:75-88, January 2012.) for my research and I found out that you are the best contact to help me get in touch with the author for clarifications of some of his methods. Please, I would really appreciate your help to get in touch with the author.

I would also need a permission from you in order to cite this paper.

Best regards,

Niyem Mawenbe Bawana

University of South Florida

College of Engineering

Dept: Electrical Engineering

Cel: +1(813) 570 3497

No Resistance can drop my Potential!

---

info.iieta Jun 20, 2019, 1:00 PM

to me

Dear Niyem Mawenbe Bawana:

Thank you for your email. Unfortunately this paper was published in 2012 and we don't have the contact info. Sorry for the inconveniences.

Best Regards,

IIETA · 2020 Scotia One, 10060 Jasper Avenue · Edmonton · AB T5J 3R8 · Canada

Tel: +1 (780) 218 9926 · Fax: +1 (780) 341 0600 · email: info@iieta.org

ABOUT THE AUTHOR

Niyem Mawenbe Bawana is a graduate student in Electrical Engineering at the University of South Florida. He received his B.S in applied physics from Université de Lomé, Togo in 2008. He served as a high school physics and chemistry teacher in Togo from 2008 to 2015. Prior to coming to the University of South Florida, he was appointed as an intern at Stellenbosch University Department of Mechanical Engineering from January to December 2015.

Niyem Mawenbe Bawana is a recipient of Fulbright and the Pafroid scholarships both funded respectively by United State Department of State, Bureau of Education and Cultural Affairs and European Union. Niyem Mawenbe Bawana is a member of the Institute of Electrical and Electronics Engineers (IEEE).